Enhancing the Performances of PV Array Configurations Under Partially Shaded Conditions: A Comparative Study

El Iysaouy Lahcen*‡, Lahbabi Mhammed **, Oumnad Abdelmajid ***

* Department of Electrical Engendering, Mohammadia School of Engineering-EMI, Mohammed Vth University in Rabat, B.P. 765 Agdal, Rabat, Morocco

** Department of Electrical Engendering, Faculty of Science and Technology, Sidi Mohammed Ben Abdellah University, B.P. 2202. Fez, Morocco.

*** Department of Electrical Engendering, Mohammadia School of Engineering-EMI, Mohammed Vth University in Rabat, B.P. 765 Agdal, Rabat, Morocco

(lahcen.eliysaouy@um5s.net.ma, lahbabi_m@yahoo.fr, aoumnad@emi.ac.ma)

‡ Corresponding Author: El Iysaouy Lahcen, Mohammadia School of Engineering-EMI, Mohammed Vth University in Rabat, Tel: +212 695623489, lahcen.eliysaouy@um5s.net.ma

Received: 26.03.2018 Accepted:11.05.2018

Abstract- In this paper, we propose to modelize and analyze the performance of some existing solar photovoltaic (PV) array configurations such as Series Parallel (SP), Bridge Link (BL), Honey Comb (HC), Total Cross Tied (TCT) and proposed configuration Sudoku. Simulations are based on complex model two-diode of solar cell using Matlab and Simulink tools. The performances of PV configurations for all configurations have been compared using P–V characteristics, power loss for different partial shading patterns. Comprehensive simulations are carried out on these configurations. The performance of proposed configuration, Sudoku, surpass the others PV configurations for the same shading patterns.

Keywords- configurations (CPV); Partial Shade; Series-parallel (SP); Bridge-Linked (BL); Honey-Comb (HC); Total-Cross-tied (TCT); Sudoku; Shorts Narrow (SN); Shorts Wide (SW); Long Narrow (LN); Wide Long (LW).

1. Introduction

It is well known that the electrical power generated by a photovoltaic (PV) module can be greatly reduced compared to the optimal conditions of production (maximum power point)[1]–[6]. Indeed, many factors, such as shading, or the temperature [7]–[10] may be about the electric production of a photovoltaic model. In this work, we are particularly interested to study the impact of shading on energy production. Further, several patterns of shading [11] will be discussed and all possible configurations of PV modules [12]–[14] will be analysed. Besides, the effect of partial shading has been extensively studied in relation to the PV module [12], [15]. Further, the impacts related to shading can be reduced using several strategies: monitoring the maximum power point produced by the PV system, also with the adoption of the converters topologies [16]–[19] and also with the best choice of the configuration of PV modules. Furthermore, we have worked on the PV modules configurations as one of the solutions that can be used in order to reduce mismatch losses. Therefore, PV systems use different configurations to achieve the desired voltage and current. Among these configurations, there are series parallel (SP), Total Cross-Tied (TCT), Honey Comb (HC), Bridge Linked (BL) and Sudoku [20]–[22]. Several researchers proposed a new model of PV configuration like single diode model [23], [24] and two-diode [25], [26] model of PV module to study and to analyze the impact of shading on different PV configurations. This last model is complex but gives the best performances [12], [27], [28]. In this work, we are especially interested to analyse the impact of the same partial shading on the performance of the power generated from the configuration PV cited above. For this, we will use the two-diodes PV model. Four types of partial shading will be presented. Then their effect in the PV characteristics will be studied, analysed and compared. The main aim is to find out the configuration that gives the best performances under the same partial shading conditions.

2. Modeling of a PV cell using the double diode model

Many electrical models are available in the literature to represent the current-voltage curves of PV cells, especially the simple model [23] based on one diode to the complex two diode model as shown in Figure 1. For simulations, we will use the two-diode model we will utilize the complex model, in order to achieve the better representation of the PV cell characteristics. Furthermore, this model has a better precision at low radiant flux. Using this model. the current-voltage characteristic is given by the following expression [25], [29].

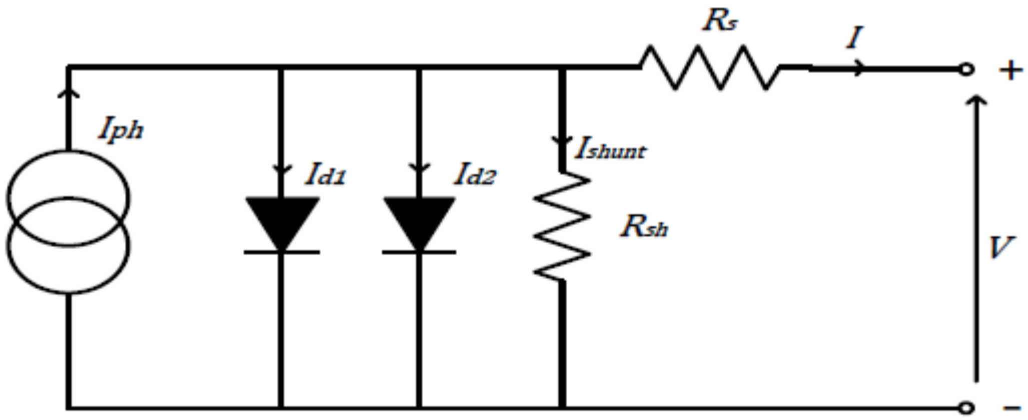

Figure 1. The model of a solar cell with two diodes.

$$I = I_{ph} - I_{s1}\left[\left(\exp^{\frac{q(V+(I\cdot Rs))}{a_1 V_{T1}}}\right)-1\right] - I_{s2}\left[\left(\exp^{\frac{q(V+(I\cdot Rs))}{a_2 V_{T2}}}\right)-1\right] - \frac{V+(I_1\cdot Rs)}{R_{sh}} \quad (1)$$

where the mathematical expression of the current Iph, the photocurrent, as follows:

$$I_{ph} = (I_{SC} + K_i(T - T_{ref})).\frac{G}{1000} \quad (2)$$

And $I_{S1,2}$ are the saturation currents respectively of the diode 1 and the diode 2 and their expression as follow:

$$I_{S1,2} = I_{rs1,2}\left((\frac{T_{ref}}{T})^3 * \left(\exp^{\frac{qEg}{a1,2}(\frac{1}{Tref}-\frac{1}{T})}\right)\right) \quad (3)$$

And $Irs_{1,2}$ reverse saturation current of the diode 1 and 2 expressed as follow:

$$Irs_{1,2} = \frac{I_{SC}}{\left(\exp^{\frac{eV_{OC}}{K.N_s.T_{ref}a_{1,2}}}\right)} \quad (4)$$

Here, $V_{T1,2}$ is the thermal voltage of the PV module. q is the electron charge, k the Boltzmann constant, T is the absolute temperature of the PN-junction in Kelvin, Ki the short-circuit current of the cell at (1000 W/ m^2, 25 °C). The variables a_1 and a_2 respectively the diffusion and recombination current components of the diodes 1 and 2. Finally, Rsh is the parallel resistance, and Rs is the series resistance.

Reference model

The modeling and simulation of the PV module represented in Figure 2 are basing on specifications of industrial PV module BP Solar MSX 60W, as given in Table 1.

Table 1. Datasheet of BP Solar MSX 60W

Specifications	value
Maximum power (Pmax)	60W
Voltage @ Pmax (Vmp)	17.1V
Current @ Pmax (Imp)	3.5A
Guaranteed minimum Pmax	58W
Short-circuit current (Isc)	3.8A
Open-circuit voltage (Voc)	21.1V
Temperature coefficient of open-circuit voltage	-(80±10) mV/°C

Temperature coefficient of short-circuit current	(0.065±0.015) %/°C

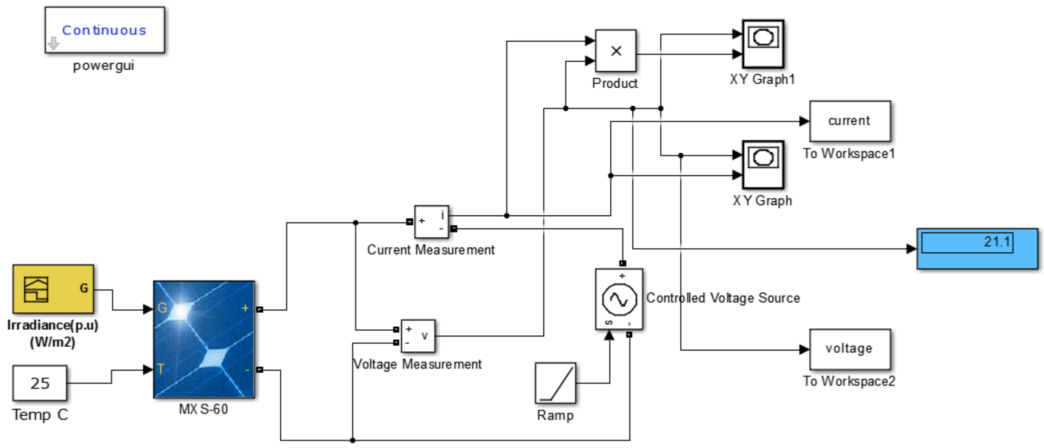

Figure 2. PV module model under STC (1000W/m^2 ,25 °C)

For the simulation, we have used the Matlab and Simulink tools. Figure 3 presents the electrical characteristics (current-voltage) I-V curved under Standard Test Conditions (STC) (1000 W/m^2, 25°C). Figure 4 displays the module's (power-voltage) P-V curved under STC.

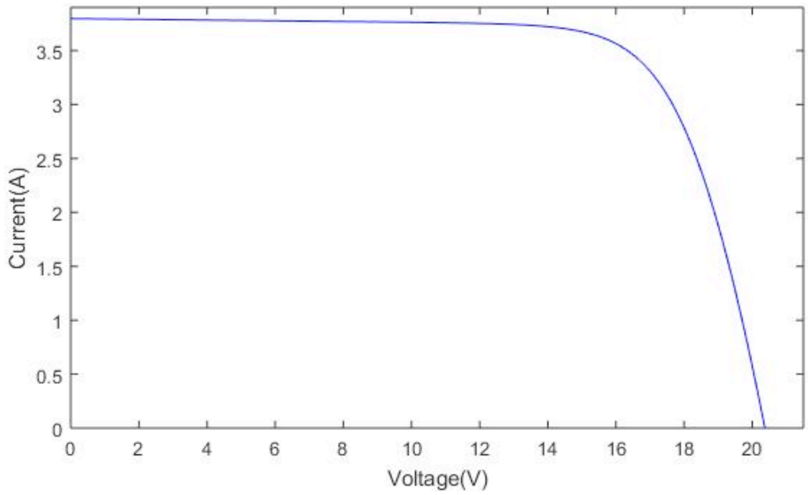

Figure 3. The output I–V curve for 1000 W/m^2 and 25 °C of PV model

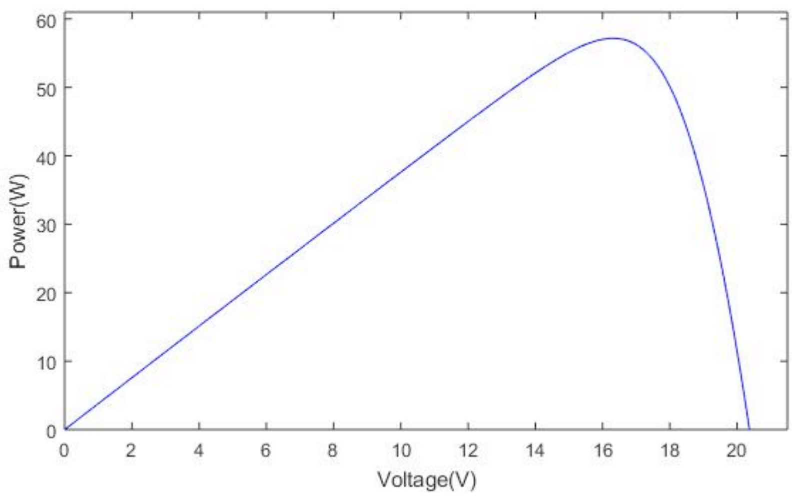

Figure 4. The output P–V curve for 1000 W/m^2 and 25 °C of PV model

3. Modeling and presentation of different PV configurations

In order to get a power of a few kW to a few MW under a suitable tension, it is necessary to connect the modules on the diverse form which is called a PV configuration. In this part, we purpose to exhibit all the PV configurations used in this study. Nevertheless, for all the simulation analyses and for all configurations results, we have used 6x4 PV modules. Each module comprises 36 cells based on the model of two diodes connected in series and shielded by a bypass diode. Moreover, we have analyzed five PV configurations as shown in the figure 5 and figure 6. The upper letters below configurations are the acronym of their names, for example SP (Series-Parallel). BL (Bridge Linked) inspired by a wheat stone Bridge connection. HC (Honey Comb) which is similar to the hexagon form of the Honey Comb [12], [21], [30]–[32]. All these PV configurations have four parallel strings and each string contains six modules connected in Series.

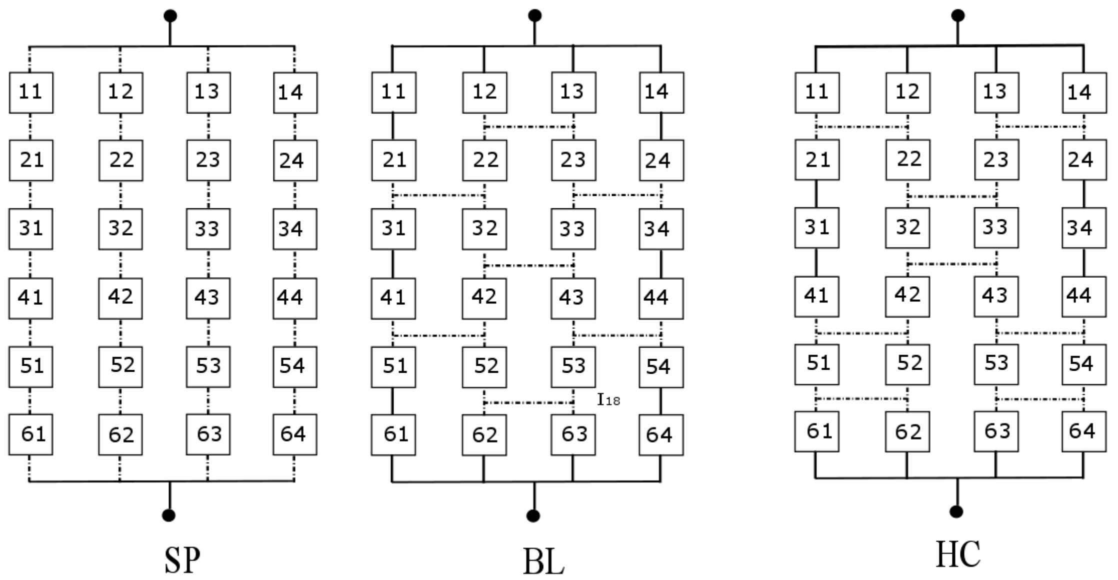

Figure 5. PV configuration, SP (Series-Parallel), HC (Honey Comb), BL (Bridge Linked).

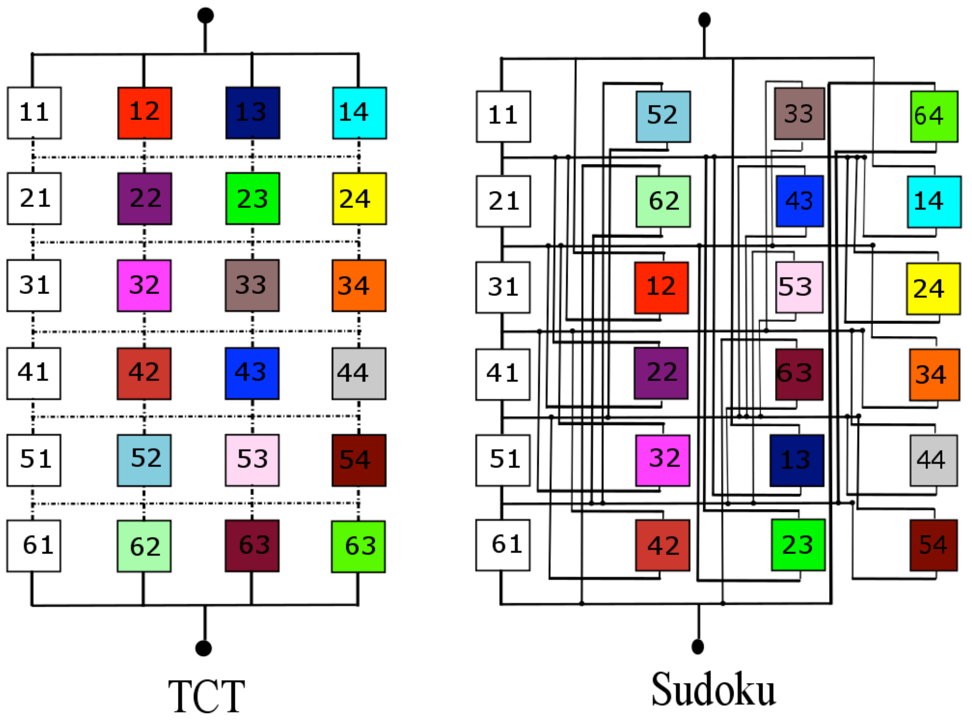

Figure 6. PV configuration, TCT, and Sudoku.

TCT (Total Cross Tied), as shown in Figure 6, having all its modules linked. Sudoku as depicted in figure 6 inspired its name from the Sudoku game, which is an improvement of TCT configuration. Sudoku basing on alteration of the row numbering of each module in a 6x4 array in order to improve the power output of the whole system under the partial shading conditions. Moreover, the column number rests the same as in the TCT topology, while the row, in which the module is physically placed, is adjusted as per Sudoku arrangement. Therefore, the electrical connections of the modules rest unchanged as in a TCT arrangement while the physical positions of the modules are the only ones altered.

4. Characteristics of shadow

The main purpose of this work is to choose a topology of PV array configuration that gives the best performance during the partial shadow. This is done through the use of the characteristics of shadow shape. The intensity of a shadow describes how much it can filter the power that glows over the PV array. This power is named irradiance and it is measured in watts per square meter. the shadow pattern can be vertical, horizontal, and diagonal. but the researchers also divided this types into another four kinds depended to the existence of the shadow in the PV array as depicted in figure 7: Shorts Narrow (SN); Shorts Wide (SW); Long Narrow (LN); Wide Long (LW). For example, when the shadow covered more than 50% of the modules vertically and less than 50 % horizontally it's called SW. If the shadow shielded less than 50% of the modules vertically and less than 50 % horizontally it's called SN. However, in this work, we have studied just one case for each kind of shadow in order to choose the PV array configuration that gives the best performance of power. It is important to note that in this work, a partial shadow is considered to be cast upon all cells of a PV module with the identical intensity. [11], [33].

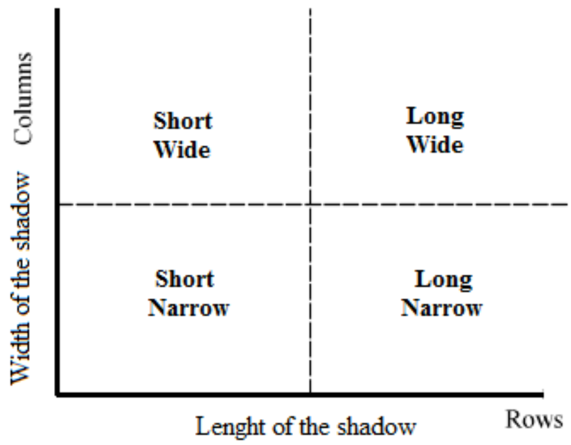

Figure 7. Four different shadow types.

The irradiations chosen to study this types of shadow are 1000 W/m^2, 324 W/m^2 and 163 W/m^2 respectively. The 1000 W/m^2 considered as an origin, STC, where the PV module can give the maximum power. The two others are chosen to represent a medium and a low extreme value of irradiations.

In order to illustrate each pattern, we have defined our PV system as finite-dimensional matrix Ln×p where $n \in IN^*$ denotes the number of modules per rows and the $p \in IN^*$ denote the number of modules per columns. The n rows are horizontal and the p columns are vertical. Each element $a_{i,j}$ {i=1 to 6 and j=1 to 4} of a matrix represented a module. For example, $a_{4,1}$ represents the module at the fourth row and first column of a matrix L. The modules are placed as follows:

$$L_{6\times4} = \begin{pmatrix} a_{11} & a_{12} & a_{13} & a_{14} \\ a_{21} & a_{22} & a_{23} & a_{24} \\ \vdots & \cdots & \ddots & \vdots \\ a_{61} & a_{62} & a_{63} & a_{64} \end{pmatrix}$$

4.1. *Pattern-1 Short Narrow (SN)*

This type can contain several shade patterns, although in this work we consider one case that received three different radiations. Therefore, the values of different irradiation for this pattern of shading are presented in the following matrix:

$$L_{6\times4} = \begin{pmatrix} 163 & 1000 & 1000 & 1000 \\ 324 & 1000 & 1000 & 1000 \\ 1000 & 1000 & 1000 & 1000 \\ 1000 & 1000 & 1000 & 1000 \\ 1000 & 1000 & 1000 & 1000 \\ 1000 & 1000 & 1000 & 1000 \end{pmatrix} \; {}^{w}\!/_{m^2} \quad at \quad 25°C$$

4.2. *Pattern-2 Short Wide (SW)*

For this kind, shading is dispersed as shown in the following matrix:

$$L_{6\times4} = \begin{pmatrix} 1000 & 1000 & 1000 & 1000 \\ 1000 & 1000 & 1000 & 1000 \\ 1000 & 1000 & 1000 & 1000 \\ 1000 & 1000 & 1000 & 1000 \\ 0163 & 0324 & 0324 & 0324 \\ 0163 & 0324 & 0324 & 0324 \end{pmatrix} \; {}^{w}\!/_{m^2} \quad at \quad 25°C$$

In this pattern, the shading exceeds the average number of modules in series for the same column and the average number of modules connected in parallel. Also, the distribution of shading must exceed an average number of modules linked in parallel.

4.3. *Pattern-3 Long Narrow (LN)*

For this pattern, two modules in series received an irradiation of 163 W/m^2 and two others connected with the first one are received an irradiation of 324 W/m^2 as shown in the matrix below.

$$L_{6\times4} = \begin{pmatrix} 1000 & 1000 & 1000 & 0163 \\ 1000 & 1000 & 1000 & 0163 \\ 1000 & 1000 & 1000 & 0324 \\ 1000 & 1000 & 1000 & 0324 \\ 1000 & 1000 & 1000 & 1000 \\ 1000 & 1000 & 1000 & 1000 \end{pmatrix} \, {}^{w}\!/_{m^2} \quad at \quad 25C°$$

4.4. *Pattern-4 Long Narrow (LW)*

The below matrix exposes the LW shading pattern. The shading for the same column exceeds the half of the modules in series and also surpasses half the average number of the modules connected horizontally.

$$L_{6\times4} = \begin{pmatrix} 1000 & 1000 & 1000 & 0163 \\ 1000 & 1000 & 1000 & 0163 \\ 1000 & 1000 & 1000 & 0163 \\ 1000 & 1000 & 1000 & 0163 \\ 0324 & 0324 & 0324 & 0324 \\ 0324 & 0324 & 0324 & 0324 \end{pmatrix} \, {}^{w}\!/_{m^2} \quad at \quad 25°C$$

5. Simulation & results

5.1. *Effect of shading on different configurations under Pattern-1 SN*

The shading in PV array configurations is divided into three groups of different modules. Each group receiving a different irradiation as shown in the matrix of pattern SN above. Moreover, the first group receives an irradiation of 1000W/m^2, the second and the third group receives an irradiation of 324 W/m^2 and 163 W/m^2 respectively. Nevertheless, the PV characteristics obtained of the five configurations TCT, Sudoku, SP, BL, and HC for this SN shading pattern are exposed in Figure 8.

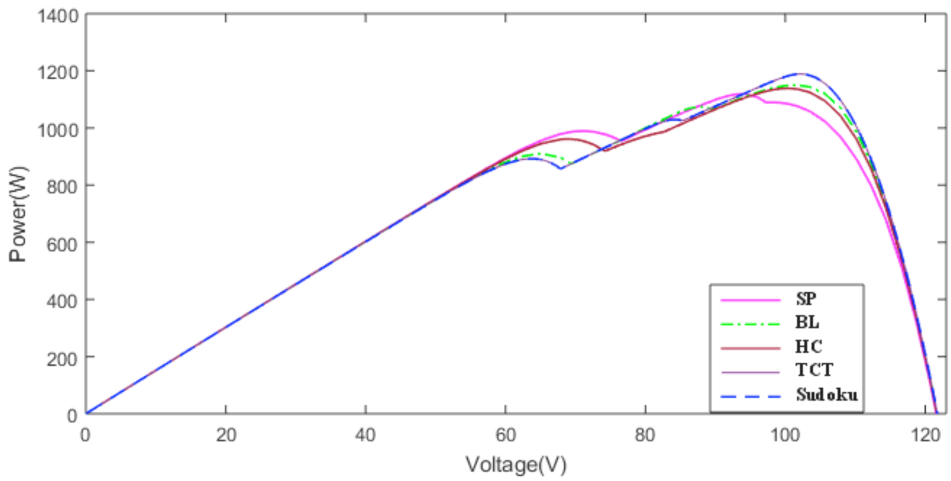

Figure 8. The output P–V curves for PV configurations in the condition SN.

Figure 8 shows that the position of the highest peak GP (global peak) is slightly increased in the topology Sudoku configuration compared to the TCT and other configurations. The results of this type of shading for different configurations are set out in Table 2. Where the PSmax is the maximum shading power and Pmax is the maximum power in case this is no shading.

Table 2. Comparison of the powers for different configurations under pattern-1SN

Configuration	PSmax (W)	Pmax (W)	Losses
SP	1119	1370	19%
BL	1139	1370	17%
HC	1135	1370	18%

TCT	1189	1372	14%
Sudoku	1189	1372	14%

The summarized results in table 2 clearly exhibit the power losses between SP, BL and HC configuration which gives almost the same performance for the SN pattern. Therefore, TCT and Sudoku configurations are improved and provided the same powers and have the same power losses, because the position of the modules does not change belonging to the first column of the TCT and Sudoku configurations.

5.2. *Effect of shading on the different configurations under Pattern-2 SW*

In this case, three different radiations are considered for calculating the performance of the PV system. The simulation results are presented in Figure 9 below.

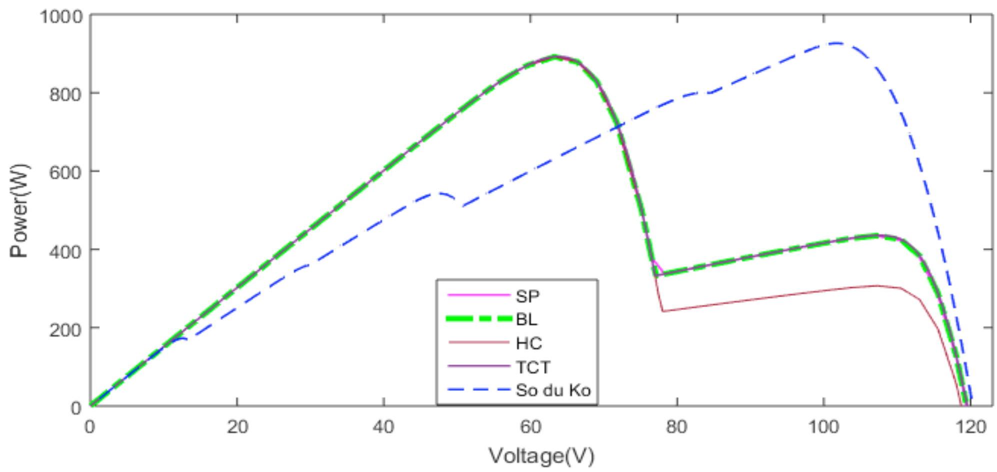

Figure 9. The output P–V curves for PV configurations under pattern-2 SW

Simulations show that there are maximum peaks and local peak in SP, TCT, HC, and BL configurations corresponding to the amount of shading caused by the partial shading SW pattern. We can note that the configuration Sudoku does not show significant changes and will be considered as best solution to solve this problem of peaks diversity. However, the amount of losses is summarized compared in Table 3 below:

Table 3. Comparison of the powers for different configurations under pattern-2 SW

Configuration	PSmax (W)	Pmax (W)	Losses
SP	891	1370	35%
BL	891	1370	35%
HC	891	1370	35%
TCT	891	1372	36%
Sudoku	925	1372	33%

This table shows that the configuration Sudoku provided the same performance, however, the comparison clearly indicates that the maximum generated power is 891W/ m^2 for TCT, SP, BL, and HC, but Sudoku is 925 W/m^2, with a slightly significant increase. This increase consequence of dispersion of shade on different tidy. The SP configurations, BL, HC generated the same losses for this partial shading pattern SW. Otherwise, the table 3 shows that the power losses are so important around 35% for all configurations.

5.3. *Effect of shading on different configurations under pattern-3 LN*

The P–V characteristics obtained in each configuration for this shading pattern LN are exposed in Figure 10. We can observe that the effect of shadowing is the same for different configuration under this kind of shadow pattern LN.

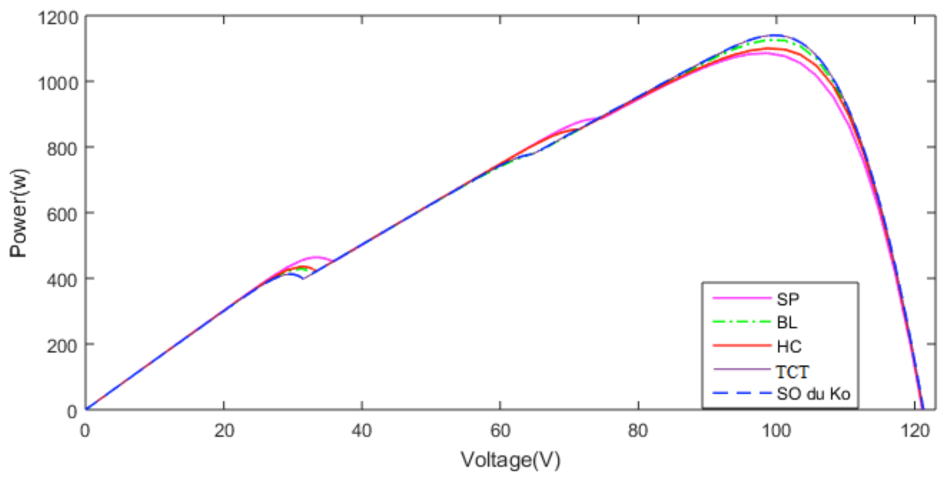

Figure 10. The output P–V curves for PV configurations under pattern-3 LN

Table 4. Power comparison of different configurations under pattern-3 LN

Configuration	PSmax (W)	Pmax (W)	Losses
SP	1086	1370	21%
BL	1126	1370	18%
HC	1100	1370	20%
TCT	1140	1372	17%
Sudoku	1140	1372	17%

5.4. *Effect of shading on different configurations under pattern-4 LW*

The P-V characteristics corresponding to shading pattern LW are shown in Figure 11. It is observed that the configuration Sudoku shows the maximum power for the LW shading pattern. While the performance of the SP, BL, HC, and TCT configurations are weakened relative to Sudoku. The comparison of the powers for different configurations under pattern-4 LW is summarized in Table 5.

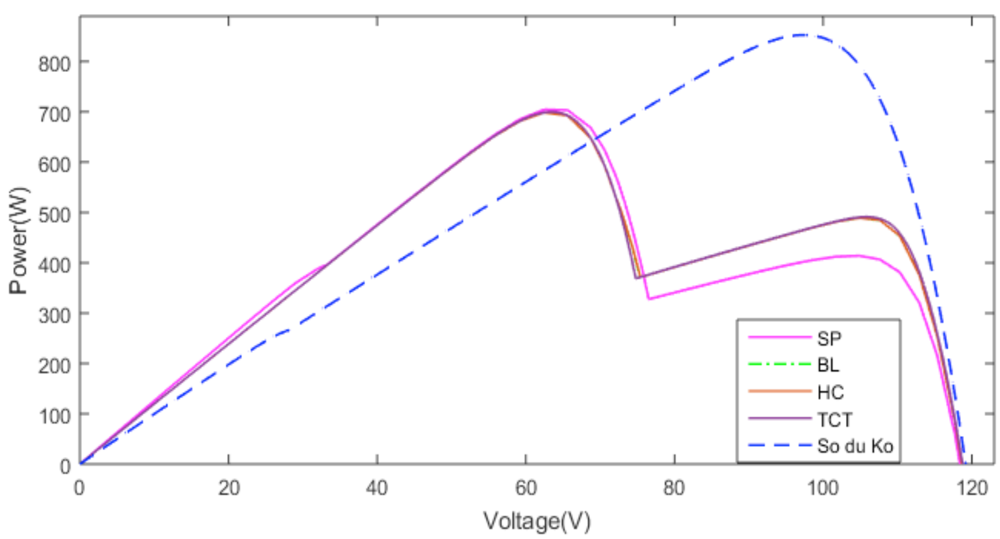

Figure 11. The P–V curves for PV configurations under pattern-4 LW

Table 5. Comparison of the powers for different configurations under pattern-4 LW

Configuration	PSmax (W)	Pmax (W)	Losses
SP	704.5	1370	48.5%
BL	698	1370	49.05%
HC	698	1370	49.05%
TCT	699	1372	49.05%
Sudoku	852.6	1372	37.85%

The configuration Sudoku providing the best power and low losses compared to other configurations SP, BL, HC, and TCT. However, the SP, BL, HC, and TCT configurations have losses can reach 50%.

6. Results and performance evaluation

The previous results for the PV configurations for different patterns are reported in Table 6. It will serve to compare the powers and powers losses for different configurations under different shadows. We can be assumed that:

- The SP, BL, HC and TCT configurations provide the same maximum powers under the pattern-2 SW.

Table 6. Maximum PV power and Power loss of different Configuration

Configuration	Pattern (SN)		Pattern (SW)		Pattern (LN)		Pattern (LW)	
	PSmax	Losses	PSmax	Losses	PSmax	Losses	PSmax	Losses
SP	1119	19%	891	37%	1086	21%	704.5	49.5%
BL	1139	17%	891	37%	1126	18%	698	49.05%
HC	1135	18%	891	35%	1100	20%	698	49.05%
TCT	1189	14%	891	37%	1140	17%	699	48.05%
Su-Do-Ku	1189	14%	925	33%	1140	17%	852.6	37.85%

- The TCT configuration the same performances as Sudoku under shadow pattern SN and pattern LN.
- The Sudoku configuration presents the best performance i.e. the lower power loss and therefore the highest maximum power under the patterns studied in this work.
- The losses for different configurations are so important in pattern LW followed by SW and then LN and SN represent the lower losses.
- The SP, BL, HC configurations provide the same power loss under the all patterns.

For more illustration of this results we have grouped them in the figure 12.

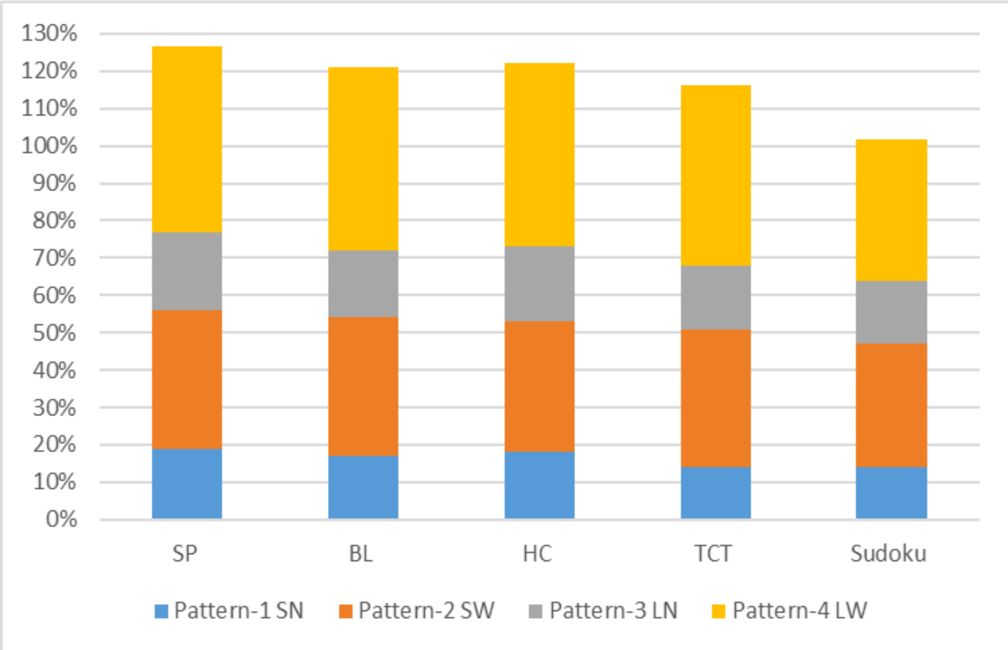

Figure 12. Maximum PV power and Power loss of different Configurations under shadow conditions

- During the partial shading Sudoku ensure the best performances, in terms of lowest power losses and highest maximum power.
- the pattern-1 SN represent lowers losses compared to the other patterns.

1. Conclusion

The performances of SP, BL, HC, TCT, and Sudoku PV array configurations under shading conditions are studied and analyzed using two-diode model under MATLAB/Simulink. We have presented different configurations and the four shadow patterns treated in this work. The obtained results exhibit the performance of Sudoku configuration which is formed based on shade dispersion in improving the overall PV performance under different pattern conditions. In fact, in Sudoku configuration, the physical position of PV modules is changed, without altering the electrical connection of modules. Nevertheless, the full analysis and studies of the configurations within various shading patterns reveal that the selection of the optimal and suitable configuration depends heavily on the nature of and the position of the shading pattern. Overall it is presumed that proposed Sudoku configuration enhance strongly the performances of PV array configurations as compared to the other PV configurations. Moreover, the results prove that this approach of Sudoku allows achieving a higher electrical performance production compared to that available PV configurations. Future works are aimed at developing an intelligent control method for the physical displacement of the PV modules under different shading pattern.

References

[1] F. Belhachat and C. Larbes, ‘Global maximum power point tracking based on ANFIS approach for PV array configurations under partial shading conditions’, *Renew. Sustain. Energy Rev.*, vol. 77, pp. 875–889, Sep. 2017.

[2] B. Bendib, H. Belmili, and F. Krim, ‘A survey of the most used MPPT methods: Conventional and advanced algorithms applied for photovoltaic systems’, *Renew. Sustain. Energy Rev.*, vol. 45, pp. 637–648, May 2015.

[3] M. A. Eltawil and Z. Zhao, ‘MPPT techniques for photovoltaic applications’, *Renew. Sustain. Energy Rev.*, vol. 25, pp. 793–813, Sep. 2013.

[4] B. Veerasamy, W. Kitagawa, and T. Takeshita, ‘MPPT method for PV modules using current control-based partial shading detection’, in *2014 International Conference on Renewable Energy Research and Application (ICRERA)*, 2014, pp. 359–364.

[5] M. Saadsaoud, abbassi H. AHmed, and K. Salah, ‘Study of Partial Shading Effects on Photovoltaic Arrays with Comprehensive Simulator for Global MPPT control’, *Int. J. Renew. Energy Res. IJRER*, vol. 6, no. 2, pp. 413–420, Jun. 2016.

[6] S. Choudhury and P. K. Rout, ‘Adaptive Fuzzy Logic based MPPT Control for PV System Under Partial Shading Condition’, *Int. J. Renew. Energy Res. IJRER*, vol. 5, no. 4, pp. 1252–1263, Dec. 2015.

[7] S. Chander, A. Purohit, A. Sharma, S. P. Nehra, and M. S. Dhaka, ‘Impact of temperature on performance of series and parallel connected mono-crystalline silicon solar cells’, *Energy Rep.*, vol. 1, pp. 175–180, Nov. 2015.

[8] F. Reis *et al.*, ‘Modeling the Effects of Inhomogeneous Irradiation and Temperature Profile on CPV Solar Cell Behavior’, *IEEE J. Photovolt.*, vol. 5, no. 1, pp. 112–122, Jan. 2015.

[9] J. J. Wysocki and P. Rappaport, 'Effect of Temperature on Photovoltaic Solar Energy Conversion', *J. Appl. Phys.*, vol. 31, no. 3, pp. 571–578, Mar. 1960.

[10] P. Singh, S. Singh, M. Lal, and M. Husain, 'Temperature dependence of I–V characteristics and performance parameters of silicon solar cell', *Sol. Energy Mater. Sol. Cells*, vol. 92, no. 12, pp. 1611–1616, Dec. 2008.

[11] N. Rakesh and T. V. Madhavaram, 'Performance enhancement of partially shaded solar PV array using novel shade dispersion technique', *Front. Energy*, vol. 10, no. 2, pp. 227–239, Jun. 2016.

[12] Y.-J. Wang and P.-C. Hsu, 'An investigation on partial shading of PV modules with different connection configurations of PV cells', *Energy*, vol. 36, no. 5, pp. 3069–3078, May 2011.

[13] R. Ramaprabha and B. L. Mathur, 'A Comprehensive Review and Analysis of Solar Photovoltaic Array Configurations under Partial Shaded Conditions', *International Journal of Photoenergy*, 2012. [Online]. Available: https://www.hindawi.com/journals/ijp/2012/120214/. [Accessed: 27-Feb-2018].

[14] S. S. Buddala, V. Devabhaktuni, and S. Vemuru, 'Architectural analysis of photovoltaic systems subjected to partial shading with a simple DC-DC step-up converter', in *2013 International Conference on Renewable Energy Research and Applications (ICRERA)*, 2013, pp. 494–498.

[15] A. S. Joshi, I. Dincer, and B. V. Reddy, 'Performance analysis of photovoltaic systems: A review', *Renew. Sustain. Energy Rev.*, vol. 13, no. 8, pp. 1884–1897, Oct. 2009.

[16] E. Bielskis, A. Baskys, and M. Sapurov, 'Single Stage Microinverter Based on Two-Switch DC-DC Flyback Converter', *Elektron. Ir Elektrotechnika*, vol. 23, no. 4, pp. 29–32, Jul. 2017.

[17] F. Ghodousipour, N. Golbon, and G. Moschopoulos, 'A DC-DC converter with dual flyback converter topology', in *Applied Power Electronics Conference and Exposition (APEC), 2013 Twenty-Eighth Annual IEEE*, 2013, pp. 1999–2004.

[18] S. Perumal, K. H. Sivanand, and J. S. Rajashekar, 'Dual Switch Forward & Flyback Converter: A Comparison'.

[19] A. Belkaid, U. Colak, and K. Kayisli, 'A comprehensive study of different photovoltaic peak power tracking methods', in *2017 IEEE 6th International Conference on Renewable Energy Research and Applications (ICRERA)*, 2017, pp. 1073–1079.

[20] S. N. Deshkar, S. B. Dhale, J. S. Mukherjee, T. S. Babu, and N. Rajasekar, 'Solar PV array reconfiguration under partial shading conditions for maximum power extraction using genetic algorithm', *Renew. Sustain. Energy Rev.*, vol. 43, pp. 102–110, Mar. 2015.

[21] P. Srinivasa Rao, P. Dinesh, G. Saravana Ilango, and C. Nagamani, 'Optimal Su-Do-Ku based interconnection scheme for increased power output from PV array under partial shading conditions', *Front. Energy*, vol. 9, no. 2, pp. 199–210, Jun. 2015.

[22] C. Lee, J. Suh, and Y. Choi, 'Comparative Study on Module Connections to Minimize Degradation of Photovoltaic Systems due to Bird Droppings', *Int. J. Renew. Energy Res. IJRER*, vol. 8, no. 1, pp. 230–237, Mar. 2018.

[23] N. M. A. A. Shannan, N. Z. Yahaya, and B. Singh, 'Single-diode model and two-diode model of PV modules: A comparison', in *2013 IEEE International Conference on Control System, Computing and Engineering*, 2013, pp. 210–214.

[24] M. T. Ahmed, T. Gonçalves, and M. Tlemcani, 'Single diode model parameters analysis of photovoltaic cell', in *2016 IEEE International Conference on Renewable Energy Research and Applications (ICRERA)*, 2016, pp. 396–400.

[25] K. Ishaque, Z. Salam, and H. Taheri, 'Simple, fast and accurate two-diode model for photovoltaic modules', *Sol. Energy Mater. Sol. Cells*, vol. 95, no. 2, pp. 586–594, Feb. 2011.

[26] M. R. Rashel, A. Albino, M. Tlemcani, T. C. F. Gonçalves, and J. Rifath, 'MATLAB Simulink modeling of photovoltaic cells for understanding shadow effect', in *2016 IEEE International Conference on Renewable Energy Research and Applications (ICRERA)*, 2016, pp. 747–750.

[27] S. Malathy and R. Ramaprabha, 'Performance Enhancement of Partially Shaded Solar Photovoltaic Array Using Grouping Technique', *J. Sol. Energy Eng.*, vol. 137, no. 3, pp. 034505-034505–5, Jun. 2015.

[28] F. Belhachat and C. Larbes, 'Modeling, analysis and comparison of solar photovoltaic array configurations under partial shading conditions', *Sol. Energy*, vol. 120, pp. 399–418, Oct. 2015.

[29] A. Bouraiou, M. Hamouda, A. Chaker, M. Sadok, M. Mostefaoui, and S. Lachtar, 'Modeling and Simulation of Photovoltaic Module and Array Based on One and Two Diode Model Using Matlab/Simulink', *Energy Procedia*, vol. 74, pp. 864–877, Aug. 2015.

[30] K. Ş. Parlak, 'PV array reconfiguration method under partial shading conditions', *Int. J. Electr. Power Energy Syst.*, vol. 63, pp. 713–721, Dec. 2014.

[31] G. Velasco-Quesada, F. Guinjoan-Gispert, R. Pique-Lopez, M. Roman-Lumbreras, and A. Conesa-Roca, 'Electrical PV Array Reconfiguration Strategy for Energy Extraction Improvement in Grid-Connected PV Systems', *IEEE Trans. Ind. Electron.*, vol. 56, no. 11, pp. 4319–4331, Nov. 2009.

[32] A. S. Yadav, R. K. Pachauri, and Y. K. Chauhan, 'Comprehensive investigation of PV arrays with puzzle shade dispersion for improved performance', *Sol. Energy*, vol. 129, pp. 256–285, May 2016.

[33] L. F. L. Villa, D. Picault, B. Raison, S. Bacha, and A. Labonne, 'Maximizing the Power Output of Partially Shaded Photovoltaic Plants Through Optimization of the Interconnections Among Its Modules', *IEEE J. Photovolt.*, vol. 2, no. 2, pp. 154–163, Apr. 2012.